Materials Science-Poland, 40(3), 2022, pp. 12-26
http://www.materialsscience.pwr.wroc.pl/
DOI: 10.2478/msp-2022-0030

sciendo

An experimental investigation of wire breakage and performance optimisation of WEDM process on machining of recycled aluminium alloy metal matrix composite

P. R. Kannan[1], K. Periasamy[2], P. Pravin[3], J. R. Vinod Kumaar[4,*]

[1]Department of Mechanical and Automation Engineering, Mahendra Engineering College (Autonomous), Namakkal (Dt), Tamil Nadu, India-637 503

[2]Department of Mechanical Engineering, Kongunadu College of Engineering and Technology, Trichy Dt, Tamil Nadu. India – 621 215

[3]Department of Mechanical Engineering, Graphic Era Deemed to be University, Dehradun, India-248 002

[4]Department of Mechanical Engineering, Mahendra Engineering College (Autonomous), Namakkal (Dt), Tamil Nadu, India-637 503

In this research, a novel aluminium metal matrix composite (AMMC) was developed using recycled aluminium alloy as a matrix with 5% alumina as reinforcement. The machining experiments were conducted by varying the input parameters such as voltage (V_s), wire feed rate (F_w), current (I_p), pulse on time (ON_T) and pulse off time (OFF_T), on wire breakage. The effect of voltage level and wire breakage frequency was analysed. The parameter combinations for machining the slot of size 5 mm width and 10 mm height with high machining rate (MR) and less surface roughness (R_a) were analysed using the CRiteria Importance Through Intercriteria Correlation (CRITIC) and simple additive weighting (SAW) methods. The wire breakage frequency is lesser at minimum peak current. The optimal parameter combination for higher MR and lower R_a is found to be at 30 V, 7 mm/min, 30 A, 120 µs (ON_T) and 70 µs (OFF_T). Analysis of variance (ANOVA) is performed to understand the significant factors affecting the WEDM process. ANOVA results predict that wire feed rate and voltage contribute 47.82% and 21.23%, respectively, to MR; and pulse on time shows a 23.06% influence on surface roughness. Scanning electron microscopy (SEM) was used to ascertain the pattern of wire breakage in WEDM, and based on the results obtained from employing this technique, it is inferred that the erosion and breakage of the wire are not instantaneous and that a cone shape is formed on the either portion of the wire.

Keywords: *zinc wire, microstructure, WEDM, alumina, current*

1. Introduction

Aluminium metal matrix composites (AMMCs) are finding application in aerospace, automobile and civil industries. The machining capability for fabricating components in AMMCs is challenging due to their intricate metal structure, an example of which is the presence of reinforcement, that reduces the cutting efficiency of the tool. The wirecut electrical discharge machining (WEDM) is used in the manufacturing industries to fabricate intricate shapes and components in difficult-to-machine materials. WEDM is a well-known unconventional machining system for manufacturing complicated shapes in difficult-to-cut materials. WEDM is mainly used in the tool room for developing tool and dies. The advantages of WEDM are non-contact type, good geometrical accuracy and efficiency. In recent years, the emergence of new sustainable materials that can offer a good range of performance has upheld the research interest in the development and application of metal matrix composites (MMCs). An overview of the literature is presented in Table 1.

In this research, the machinability of scrap aluminium alloy-based composites is machined using WEDM, and this study paves way for reusability and sustainable product development. In general, the alloy wheel already consists of silicon and mag-

* E-mail: jrvinod@gmail.com

Table 1. A brief overview of the literature

S. No.	Process parameters considered	Work material investigated	Work description	Outcome of the investigation
1	Pulse on time, pulse off time, wire feed rate, current, voltage, thermal conductivity, coefficient of thermal expansion, density and wire tension [1]	Al 2124 SiCp MMCs	In the WEDM of AlSiCp MMC, DA and ANN-based predicted models for surface roughness and MRR were developed.	With an increase in pulse duration and thermal conductivity, the rate of material removal and surface roughness both increase significantly. The ANN approach gives a better result than DA.
2	Pulse on time, pulse off time and wire feed [2]	HEA-reinforced aluminium metal–metal composite	The best parameter combination for a better surface finish, a faster MRR and a smaller KW is found using the Taguchi method and an L_{18} OA.	The pulse ON time has a significant influence on surface roughness (76.70%), KW (41.96%) and MRR (35.37%), and increasing the pulse ON time enhances the response variables. According to results of multi-objective optimisation using the TOPSIS methodology, MRR and surface finish have improved while KW has significantly decreased.
3	Pulse on time, pulse off time, wire feed, wire tension, current and voltage [3]	AA6061-TiB_2	Studied the effect of reinforcement and wire material on the surface roughness in MMCs. The experiments were carried out using the Taguchi methodology. XRD analysis was used to determine the phase constituents of the work material.	The results of the experiments show that the percentage of particle reinforcement was the most important factor in surface quality (62.04%) and machinability (34.2%). The machinability and surface quality of the TiB_2 (5 wt.%) reinforced composite are excellent. Zinc-coated brass wire outperforms plain brass wire.
4	Pulse on time, pulse off time, wire feed and wire tension [4]	SiCp/Al composite	Prepared casted, coated, annealed and plastic processed wire for WEDM of MMCs.	The use of zinc coating on the wire resulted in increased MRR by 16.67%, reduced surface roughness by 21.18% and reduced wire breakage by 16.67% under the same discharge parameters when compared to brass wire electrode.
5	Short pulse time, wire feed rate, pulse width, spark gap, servo control mean reference voltage and time between pulses [5]	Al/ZrO_2 (p)-metal matrix composite	Surface veracity aspects such as surface defects and recast layer thickness are investigated.	The result finding shows lower value of pulse on/off time, and frequency of pulse plays an important role in surface veracity.
6	Gap voltage, wire feed, pulse on time and pulse off time [6]	Al-Si12/B_4C/fly ash	In WEDM of Al-Si12/B_4C/fly ash composites, the effects of control parameters on MRR and surface roughness were examined using the Taguchi and ANOVA methods.	MRR increases as the pulse on time and reinforcement increase. Optimal machining conditions resulted in a maximum MRR of 38.01 mm^3/min and a minimum surface roughness of 3.24 m.
7	Voltage, peak current, wire tension and dielectric pressure [7]	AMMCs with 6% and 8% weight fraction of Al_2O_3	AMMC with weight fraction of Al_2O_3 is machined through WEDM	Based on the TOPSIS approach, the optimal MR and Ra process parameters were ascertained as 1.5 mm/min and 3.648 m, respectively. According to ANOVA, the peak current has a significant influence on MR and Ra.
8	Pulse on time and pulse off time, gap voltage, peak current and wire feed [8]	Aluminium-based composite materials (AA 7075) with (Al_2O_3) particles	The effect of wirecut EDM process parameters on MRR and surface roughness of Ni-P-coated and un-coated alumina-reinforced composite materials was investigated.	By combining grey relation analysis with principal component analysis, an ideal set of process parameters was observed. The identified optimal parameters were validated by running confirmation tests, and the experimental results were observed to be in good agreement with the predicted results.
9	Pulse on time and pulse off time, gap voltage, reinforcement and wire feed [9]	LM5/ZrO_2 AMMCs	By using the Taguchi technique, the study sought to determine the optimal wire-EDM machining parameters for achieving maximum MRR, minimum SR and minimum kerf width KW.	The main statistical factors influencing MRR are the gap voltage (29.92%) and pulse on time (64.84%).
10	Pulse on time and pulse off time, gap voltage, percentage of reinforcement and wire feed [10]	Aluminium (LM25) reinforced with fly ash and boron carbide (B_4C) hybrid composites	WEDM experiments were planned and carried out using the Taguchi methodology's L_{27} OA approach, and the corresponding MRR and surface roughness were measured.	The grasshopper optimisation algorithm performed better than the others in terms of maximising volume removal rate and minimising surface roughness values, according to the results.

11	Doping percentage, reinforcement percentage, pulse on time and pulse off time, and wire feed [11]	Magnesium MMC	Investigation in WEDM has been carried out to oversee the effect of process variables on the machining performance parameters such as MRR and Ra of magnesium composite.	The results of the experiment show that increasing the duration of pulse ON and wire feed rate in WEDM increases the MRR. Surface roughness increases noticeably as pulse ON increases.
12	Cutting speed, feed and depth of cut [12]	Aluminium (AA6061) and alumina powder sized <1 mm with 99.9% purity	The study investigated the effects of varying alumina amounts ranging from 1 wt.% to 5 wt.% added to recycled aluminium chip using hot press forging. Ultimate tensile strength and elongation to failure were the primary responses studied.	The addition of 2 wt.% alumina to the recycled aluminium alloy produced high-quality and consistent results.
13	Current, pulse on time, wire speed, voltage and pulse off time [13]	SiCp reinforced Al6061 composite	The effect of parameters such as current, pulse on time, wire speed, voltage and pulse off time on wire-EDM machining of 4–8 wt.% SiCp/Al6061 alloy was investigated.	MRR was significantly influenced by current, pulse on time, pulse off time, wire speed and voltage. The MRR increased as the current, pulse on time, wire speed and voltage increased, but it decreased as the pulse off time and wire speed exceeded 700 rpm.
14	Stirring temperature, stirring speed, stirring time, preheat temperature of reinforced particles, preheat temperature of permanent die and squeeze pressure [14]	AlSi7Mg + alumina; scrap aluminium alloy + alumina; AlSi7Mg + SAC; scrap aluminium alloy + SAC	In the present study, stir-squeeze casting was successfully used to create AMCs using a novel method. The viability of using SAC from oil refineries as reinforcement material and SAAWs as the matrix material was examined.	According to the micrograph analysis, the scrap aluminium alloy alumina composite had the most uniform distribution of reinforcements and the lowest porosity among the four composites.
15	Current, pulse on time, wire feed rate, pulse off time, ultimate tensile strength and micro hardness [15]	AZ61 magnesium alloy with boron carbide and silicon carbide as an reinforcement with varying percentage levels	The fabricated magnesium MMC is machined through WEDM for MRR and surface roughness.	The highest MRR of 0.212 mm^3/s was obtained at pulse on time of 115 µs and pulse off time of 50 µs, and the minimum values of surface roughness were obtained as 1.003942 µm.
16	Alumina weight percentage, amplitude percentage and pulse time [16]	SAAWs	Using a L_9 OA and the Taguchi method, an experimental study was carried out. Multi-objective optimisation based on ratio analysis technique was used for optimisation.	The findings showed that compared to other composites, SAAWs reinforced with 1 weight percent of nanosized alumina particles and 5.5 weight percent of micro sized alumina particles had lower porosity and metal loss (wear), higher hardness, tensile strength, and compressive strength.
17	Cutting speed, surface topography, surface roughness, recast layer formation, residual stresses and microstructural and metallurgical alterations [17]	Inconel 706	To determine the feasibility of machining these components, research was carried out on Inconel 706 superalloy using the WEDM process.	Despite the fact that zinc-coated wire improves productivity, hard brass wire was noticed to be advantageous in terms of improved surface quality of machined parts.
18	Pulse off time, pulse on time, gap voltage and peak current [18]	[Difficult-to-cut materials]	The study concentrated on the impacts of various optimisation techniques, such as single and multi-objective techniques, on difficult-to-cut materials.	Reviewed the recent and early research articles on the WEDM process to cut hard conductive materials along with single response and multi response optimisation.
19	Pulse off time, pulse on time, gap voltage and peak current [19]	A286 superalloy	Optimised the WEDM performances by particle swarm optimisation.	The best MRR and surface roughness, respectively, were 19.90 mm^2/min and 3.49 m.
20	Pulse off time, pulse on time, gap voltage and peak current [20]	Hard-to-cut materials	Six algorithms, namely MOALO, NSMFO, MODA, MOGWO, MOGOA and NSWOA, are used in the Pareto optimisation of a WEDM process.	The results reveal that MOGWO, MOGOA and MODA can identify the optimum solutions in 47%, 28% and 20% of the situations, respectively.

AMMCs, aluminium metal matrix composites; ANN, artificial neural network; ANOVA, analysis of variance; DA, dimensional analysis; KW, kerf width; MMC, metal matrix composite; MOALO, multi-objective ant lion optimisation; MODA, multi-objective dragonfly algorithm; MOGOA, multi-objective grasshopper optimisation algorithm; MOGWO, multi-objective grey wolf optimiser; MRR, material removal rate; NSMFO, non-dominated sorting moth flame optimisation; NSWOA, non-dominated sorting whale optimisation algorithm; OA, orthogonal array; SAAWs, scrap aluminium alloy wheels; SAC, spent alumina catalyst

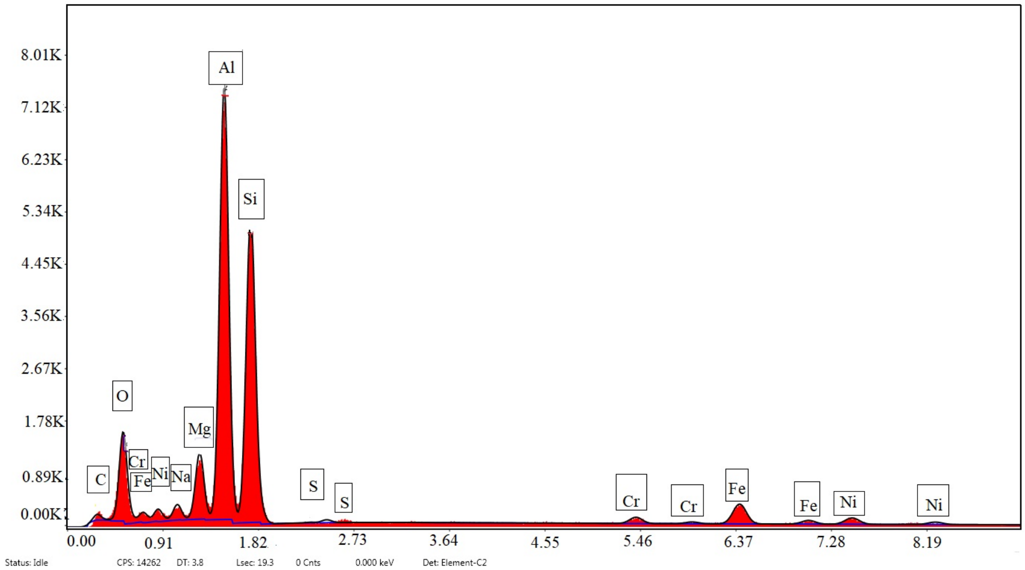

Fig. 1. EDX analysis of AMMC. AMMC, aluminium metal matrix composite; EDX, energy-dispersive X-ray

Table 2. Chemical compositions of composite materials

Element	**Weight percentage**	**Atomic percentage**	**Error percentage**
C K	4.49	9.08	21.36
O K	16.53	25.11	9.43
Na K	1.86	1.96	11.36
Mg K	5.01	5.01	6.53
Al K	31.72	28.58	4.71
Si K	29.47	25.5	6.15
S K	0.07	0.05	29.63
Cr K	1.44	0.67	12.35
Fe K	6.53	2.84	5.11
Ni K	2.9	1.2	10.1

nesium, and addition of Al_2O_3 greatly improves the mechanical properties of the material. AMMCs is finding applications in various industries such as aerospace, marine and automobile, primarily in the body structure. The machining of AMMCs becomes an essential area of research due to the above applications. In this research, the performance of zinc-coated wire on AMMC was analysed through experimental performance by varying one parameter at a time and characterisation using scanning electron microscopy (SEM) and energy-dispersive x-ray spectrometry (EDS). Moreover, the L_{18} orthogonal array (OA) experimental design is considered to find the optimal combination of factors using the CRiteria Importance Through Intercriteria Correlation (CRITIC) and simple additive weighting (SAW) methods, and the significant factor affecting the WEDM process is ascertained using the ANOVA method.

2. Materials and methods

Electronic Computer Numerical Control (CNC) WEDM is used for making slots on the fabricated MMCs. A zinc-coated brass wire electrode of Φ 0.25 mm is used for the cutting. The zinc coating improves the flushability and instant cooling ability of the wire [15]. The workpiece is formed from the scrap aluminium alloy wheels (SAAWs) of vehicles as a matrix and 5% alumina as reinforcement.

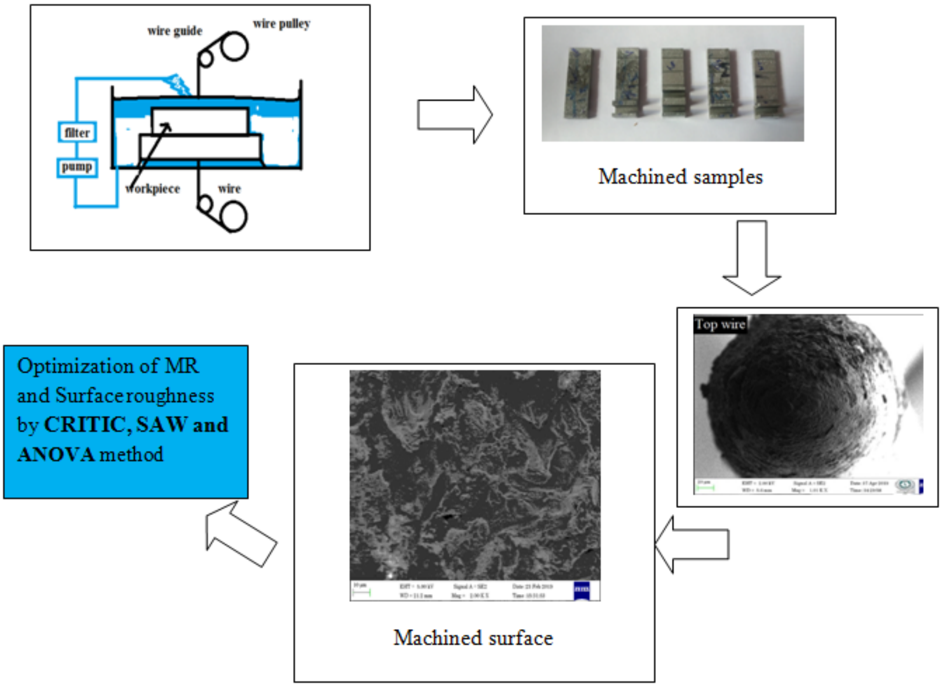

Fig. 2. Overview of the experimental work and methodology. ANOVA, analysis of variance; CRITIC, CRiteria Importance Through Intercriteria Correlation; MR, machining rate; SAW, simple additive weighting

Table 3. Control variables and their levels

Control variables	Symbols	Units	Level 1	Level 2	Level 3	Level 4	Level 5
Voltage	V	V	30	40	50	60	70
Wire feed rate	F_w	mm/min	3	4	5	6	7
Current	I_p	A	10	15	20	25	30
Pulse on time	ON_T	µs	100	105	110	115	120
Pulse off time	OFF_T	µs	50	55	60	65	70

The AMMCs are fabricated through stir-squeeze casting technique. The SAAWs of necessary size are melted in an electric furnace on a graphite crucible and heated to a temperature of 900°C. To enhance the wettability among the matrix and the reinforcements, magnesium of 1wt.% is added to the melt. A two-blade stirrer is used for 5 min to mix the molten metal to ensure uniform mixing of reinforcement in the Al matrix. The molten mixture is poured into a permanent mould of dimensions 50 mm× 50 mm× 250 mm and cooled and solidified at room temperature. The workpiece consists of recycled aluminium alloy reinforced with silicon and magnesium, and the chemical composition of the workpiece is confirmed using energy-dispersive X-ray spectroscopy (EDS) analysis, as shown in Figure 1 and in Table 2. Deionised water is used as the dielectric medium. The material is removed by a sequence of discrete discharges between the wire electrode and the workpiece in the presence of dielectric fluid, which creates a path for each discharge as the fluid becomes ionised in the gap. The area where discharge takes place is heated to a tremendously high temperature, so that the surface is melted and removed [16–18]. The removed particles are flushed away by the flowing dielectric fluids.

The experimental variables, namely voltage (V_s), wire feed rate (F_w), current (I_p), pulse on time (ON_T) and pulse off time (OFF_T), were selected

Table 4. Performance measure of wire breakage

Ex. No.	V	F_w	I_P	ON_T	OFF_T	First incidence of wire breakage in seconds
1	30	7	30	120	70	304
2	40	7	30	120	70	60
3	50	7	30	120	70	32
4	60	7	30	120	70	27
5	70	7	30	120	70	22
6	70	3	30	120	70	-
7	70	4	30	120	70	28
8	70	5	30	120	70	21
9	70	6	30	120	70	19
10	70	7	30	120	70	15
11	70	7	10	120	70	727
12	70	7	15	120	70	32
13	70	7	20	120	70	26
14	70	7	25	120	70	23
15	70	7	30	120	70	21
16	70	7	30	100	70	1114
17	70	7	30	105	70	847
18	70	7	30	110	70	30
19	70	7	30	115	70	25
20	70	7	30	120	70	19
21	70	7	30	120	50	120
22	70	7	30	120	55	90
23	70	7	30	120	60	8
24	70	7	30	120	65	7
25	70	7	30	120	70	6

Table 5. Parameters and their levels chosen for optimisation

Control variables	Symbols	Units	Level 1	Level 2	Level 3
Voltage	V	V	30	50	70
Wire feed rate	F_w	mm/min	3	5	7
Current	I_p	A	10	20	30
Pulse on time	ON_T	µs	100	110	120
Pulse off time	OFF_T	µs	50	60	70

for the purpose of machining. Machining time is recorded for each experimental combination, and time duration for breakage of wire is noted. The input variables and levels are provided in Table 3. Each control variable is analysed at five levels to determine the wire breakage for the WEDM process. Table 4 presents the scheme of the conducted experiment and first incidence of wire breakage in seconds, corresponding to the fabrication of a slot of the size 5 mm $\times$ 10 mm. Figure 2 shows the overview of workplan and methodology.

Table 5 presents the levels and parameters used for the performance optimisation of WEDM process. Machining rate (MR) and surface roughness (R_a) are considered as performance measures. Five parameters at the third level are considered for this experiment, and accordingly 10 applicable degrees of freedom are used; resultantly, L_{18} OA is considered for executing the experiments, as indicated in Table 6.

Table 6. L_{18} OA

Exp. No.	V	F_w	I_p	ON_T	OFF_T	MR mm/min	Surface roughness (R_a) μm
1	30	3	10	100	50	1.02	3.600
2	30	5	20	110	60	1.02	3.795
3	30	7	30	120	70	1.52	3.748
4	50	3	10	110	60	0.9	3.218
5	50	5	20	120	70	1.25	3.789
6	50	7	30	100	50	1.24	3.780
7	70	3	20	100	70	1.04	3.392
8	70	5	30	110	50	0.85	3.392
9	70	7	10	120	60	1.06	3.722
10	30	3	30	120	60	0.85	3.570
11	30	5	10	100	70	1.28	3.575
12	30	7	20	110	50	1.35	3.405
13	50	3	20	120	50	0.82	3.532
14	50	5	30	100	60	0.92	3.420
15	50	7	10	110	70	1.23	3.228
16	70	3	30	110	70	0.76	3.729
17	70	5	10	120	50	0.88	3.686
18	70	7	20	100	60	1.06	3.370

OA, orthogonal array

2.1. CRITIC and SAW method optimisation

The CRITIC weighting method deals with the interdependence between the criteria. The CRITIC method is more appropriate for weighing up the weights of both conventional and modern performance measures, and it comprises all the information in the assessment criteria. Moreover, the SAW method is used to compute the index score.

The weights of the criteria play an essential role in deciding the actual degree of a criterion's control. In describing the output performance of WEDM, the indicator with the maximum weight is considered as the most significant indicator, and against this conceptual background, this research used the CRITIC weighting method to establish the weights of the MR and surface roughness by using the following steps:

Step 1: The normalisation of the decision matrix is represented in Eq. (1), where Z_{pq} stands for the observation of MR and surface roughness:

$$\overline{Zpq} = \frac{Zpq - Zpq^{\min}}{Zpq^{\max} - Zpq^{\min}} \quad (1)$$

$$(\text{or})\,\overline{Zq} = \frac{Zpq - Zpq^{\min}}{Zq^{\max} - Zq^{\min}}$$

$$\overline{Zpq} = \frac{Zpq^{\max} - Zpq}{Zpq^{\max} - Zpq^{\min}} \quad (2)$$

$$(\text{or})\,\overline{Zq} = \frac{Zpq^{\max} - Zpq}{Zpq^{\max} - Zpq^{\min}}$$

Step 2: Find the standard deviation σ_q for indicator q.

$$\sigma q = \sqrt{\sum \frac{(zp-\beta)^2}{K}} \quad (3)$$

Step 3: Find the symmetrical matrix $k \times k$ with the element s_{qr}, which represents the linear correlation coefficient between the vectors z_q and z_r, respectively.

$$sqr = \frac{k\sum_{n=1}^{k} qnrn - \sum_{n=1}^{k} qn \sum_{n=1}^{k} rn}{A-B} \quad (4)$$

where

$$A = \sqrt{k\sum_{n=1}^{k} sn^2 - \left(\sum_{n=1}^{k} sn\right)^2}$$

$$B = \sqrt{k\sum_{n=1}^{k} rn^2 - \left(\sum_{n=1}^{k} rn\right)^2}$$

Step 4: Next, evaluate the contradiction that criterion q creates within the context of the decision scenario described by the remaining criterion, which is evaluated by the formula represented below in Eq. (5).

$$\sum_{r=1}^{j} (1 - S_{qr}) \quad (5)$$

$$d_q = \sigma_q(*) \sum_{r=1}^{j} (1 - S_{qr}) \quad (6)$$

With regard to each criterion, determine the quantity of information as well.

Finally, the following expression in Eq. (7) below represents the objective weight for indicator q:

$$w_q^{obj} = \frac{d_q}{\sum_{r=1}^{j} d_q} \quad (7)$$

where w_q^{obj} refers to the objective indicator for the q^{th} indicator.

To optimise the MR and surface roughness, this paper proposes to use the SAW method, as given in Eq. (8):

$$B_p = \sum_{q=1}^{j} w_q \overline{(z_{pq})} \quad (8)$$

where w_q refers to the weighted value for the indicator q and $\overline{zpq}$ refers to the normalised values of MR and surface roughness.

The greatest value B_p denotes the highest ranking for MR and surface roughness.

3. Results and discussion

3.1. Analysis of Wire-EDM machined surface and wire

Figure 3 shows the effect of voltage on time for the first incidence of wire breakage while machining the slot in MMC. It is evident from the graph that at the parameter level of 30 V, 7 mm/min, 30 A, 120 µs (ON_T) and 70 µs, the first incidence of wire breakage has occurred at 304 s, before the completion of the slot. At this instance, the slot dimension for the height is measured using a Vernier height gauge and marked height of 9.4 mm. It is clear that there is a shortage in the height by - 0.6 mm, thereby not allowing the completion of the slot. At a lower voltage level, there is a greater availability in the pulse on-current for machining, and accordingly the rapid movement of material is introduced in order to ensure slot completion. Increasing the voltage from 40 V to 70 V increases the production of gas bubbles, together with the bowing effect of the wire triggering the breaking of the wire. Moreover, in the WEDM process, the wire gap condition is also an important factor that decides the efficiency of machining. During the WEDM process, the presence of reinforcement varies the gap based on the agglomeration of reinforcement. During the higher voltage levels, the presence of clusters of reinforcements can be attributed to bulk removal material and sharp reinforcement existing in the delaminated areas, and, consequent to exposure to wire, these are the areas that are the first to initiate the damage; and as a result of this effect, the wire electrode experiences breakage for the higher voltage levels. The graph trend of Figure 3 shows that at 30 V, it took a long time for the breakage of wire to occur, and with an increase in the voltage level, a frequent failure in wire was noticed. Figures 4A and 4B show the SEM images of the machined surface of the completed slot. The complete machined surface shows a few occurrences of the Al_2O_3 and re-solidified areas. The sparse presence of Al_2O_3 prevents any encounter between the material used as reinforcement and the wire, thereby facilitating the completion of the slot.

Figures 5A and 5B show the SEM picture of wire before and after machining, and it is evident

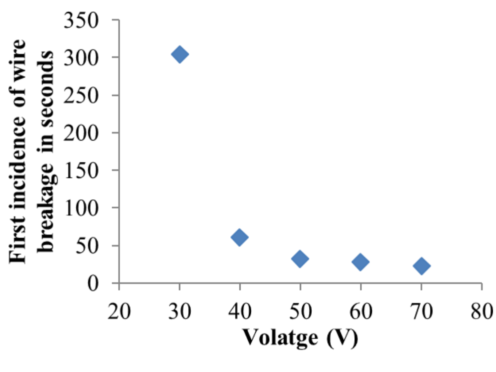

Fig. 3. Effect of voltage on the first incidence of wire breakage at 7 mm/min, 30 A, 120 µs (ON_T) and 70 µs

(A) (B)

Fig. 4. **(A, B)** SEM image of machined surface at 30 V, 7 mm/min, 30 A, 120 µs and 70 µs. SEM, scanning electron microscopy

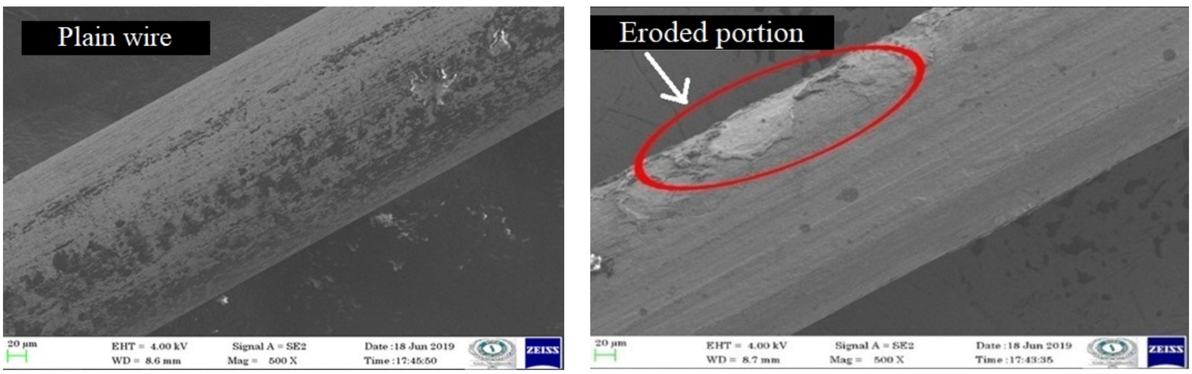

(A) (B)

Fig. 5. **(A, B)** SEM images of wire electrode surface after completing machining of the slot at conditions of 70 V, 3 mm/min, 30 A, 120 µs (ON_T) and 70 µs. SEM, scanning electron microscopy

that no significant changes are observable, except for a small quantity of erosion and re-solidified surfaces. The condition of the wire confirms efficient machining for the parametric combination of 30 V, 7 mm/min, 30 A, 120 µs (ON_T) and 70 µs.

The primary parameter that significantly influences the WEDM process is the wire feed rate. The effect of wire feed rate on the machinability of a slot in AMMC is shown in Figure 6. As can be clearly observed from the graph, we have confirmation that usage of the discussed experimental combination of input parameters—i.e., 30 V, 3 mm/min, 30 A, 120 µs (ON_T) and 70 µs—facilitates the completion of the slot without breakage of the wire, and the time taken to machine the slot is found to be 435 s. It is evident from the graph that the lower wire feed rate ensures the completion of machining of the slot without wire breakage. During the lower wire feed rate, high current passes through the wire, which allows the creation of sparks when it gets close to the conductive workpiece. Each spark is prolonged for few seconds, resulting in excess temperature, which is high enough to melt and evaporate the workpiece material. The higher electrical parameters and lower wire feed rate contributed to non-breakage of the wire. From this graph, it is evident that the wire breakage frequency increases with an increase in wire feed (F_w). The increase in wire feed rate from 3 mm/min to 4 mm/min shows a notable change in the wire breakage, and a further increase from 4 mm/min to 7 mm/min increases the frequency of the wire breakage. Figures 7A and 7B show the SEM image of the eroded and broken wire of the top and bottom portions, at the experimental condition of 70 V, 7 mm/min, 30 A, 120 µs and 70 µs. It is clear from the figure that the erosion and breakage of the wire is not instantaneous, and that a cone shape is formed on either portion of the wire. It is noted that the centre portion of the wire shows no evidence of a melted zone and occurrence of breakage is envisaged due to weakening of mechanical properties. The presence of protruding sharp-edged Al_2O_3 on the workpiece surface after melting of matrix material creates the shearing effect on the wire.

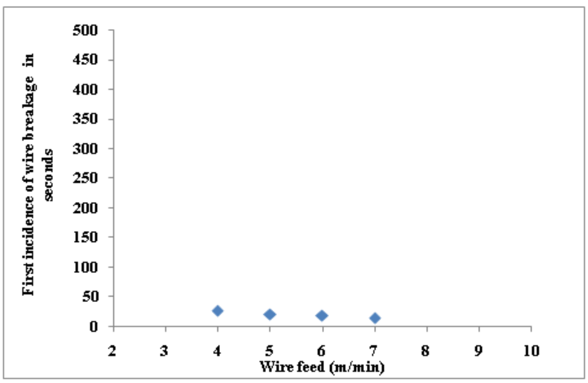

Fig. 6. Wire behaviour effect between wire feed and first incidence of wire breakage

In WEDM, zinc-coated wire electrode occupies a considerable percentage of the machining cost. Therefore, to attain stable machining without wire breakage, it is required to set a low wire feed rate and a higher level of electrical parameters.

Figure 8A shows the SEM picture of the machined surface at the parametric combination of 70 V, 3 mm/min, 30 A, 120 µs (ON_T) and 70 µs. The higher-level values of voltage, current and pulse on/off time create the high-density sparks that in turn create craters and pits. Figure 8B shows the rapidly melted and solidified regions on the surface

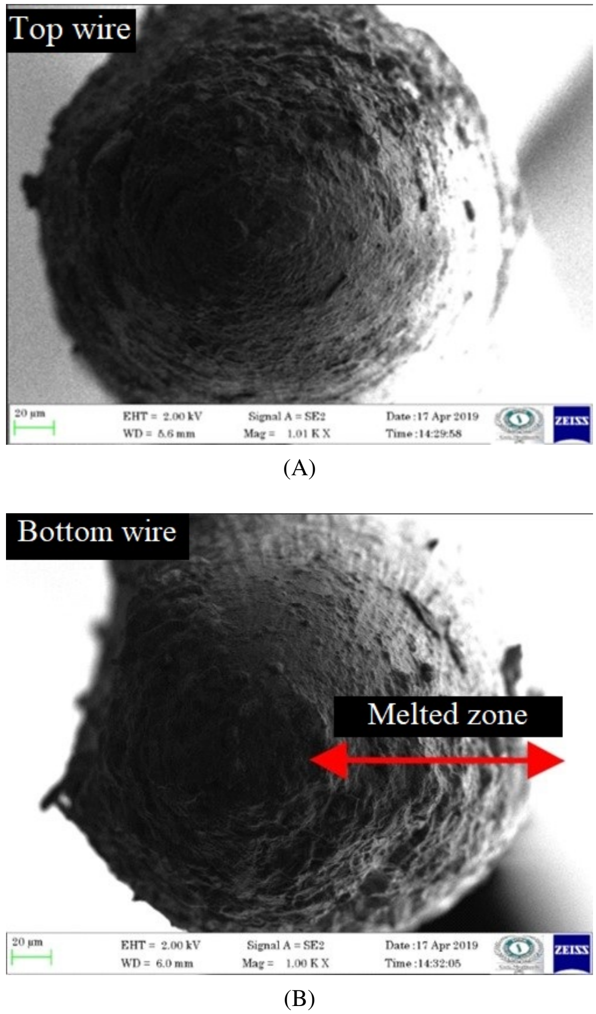

Fig. 7. Cross-sectional view of the eroded and broken wire: **(A)** top portion and **(B)** bottom portion at 70 V, 7 mm/min, 30 A, 120 µs (ON_T) and 70 µs

of the slot. Hence, the low feed rate ensures stable machining.

Figure 9 demonstrates that if we consider the applicable wire breakage as the one corresponding to the lowest value of peak current (30 A), 727 s is obtained as the time taken to machine the slot up to a depth of 9.8 mm. Increase in peak current increases the rate of heat energy. Melting and vaporisation of the wire occur at a rapid rate during the continuous increment of peak current, thereby leading to wire breakage during machining. The peak current governs the maximum amount of amperage for machining the workpiece. Roughing operations are possible with the flow of high current,

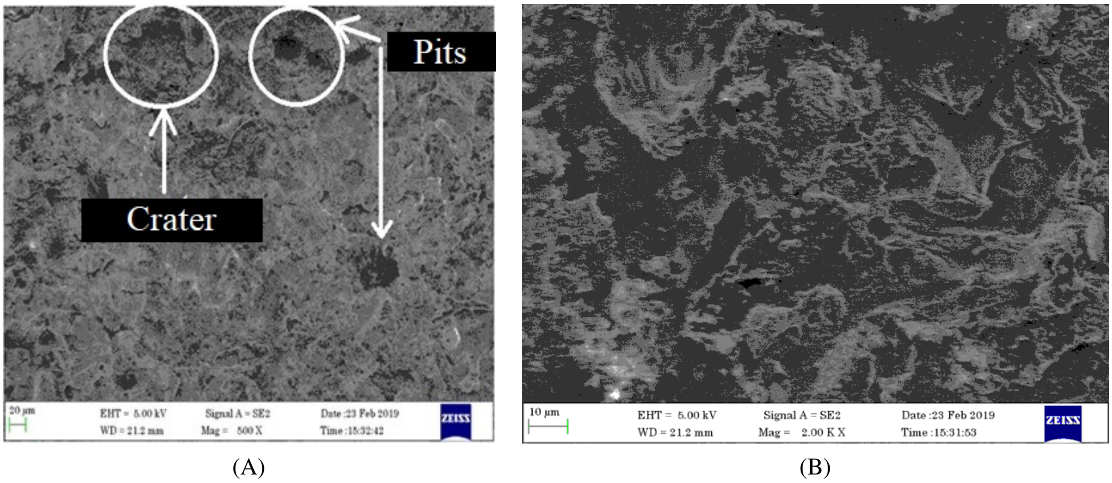

Fig. 8. **(A,B)** SEM image of machined surface at the parametric combination of 70 V, 3 mm/min, 30 A, 120 µs (ON_T) and 70 µs. SEM, scanning electron microscopy

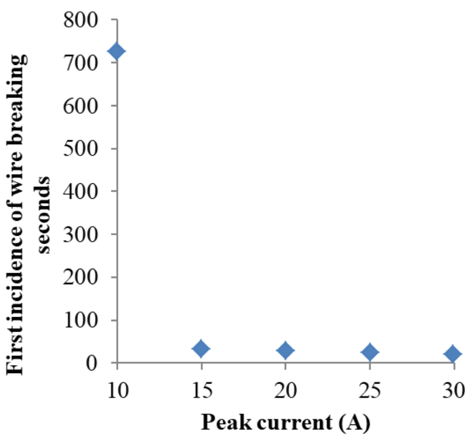

Fig. 9. Effect of peak current on the first occurrence of wire breakage

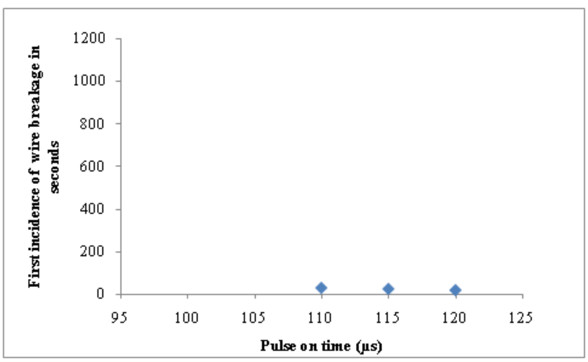

Fig. 10. Wire behaviour effect for various pulse on time

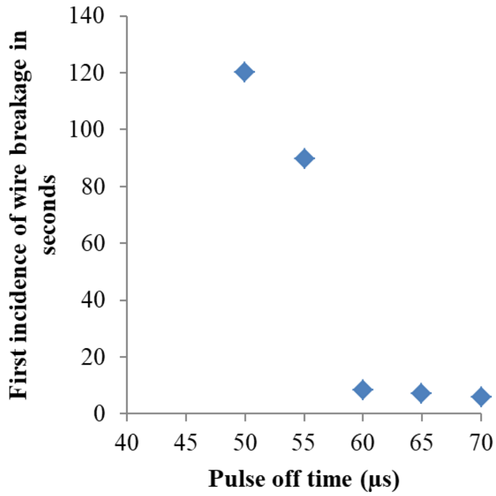

Fig. 11. Effect of pulse off time on the wire behaviour (70 V, 7 mm/min, 310 A and 120 µs [ON_T])

but they may lead to the creation of cavities. Continuous increment of peak current improves MR but reduces the surface roughness. In AMMC, the continuous increment of peak current leads to increasing frequency of wire breakage.

Figure 10 indicates the effect of pulse on time on the wire breakage during the machining of MMCs. The two slots were successfully completed without wire breakage at 1,115 s and 847 s. Further increase in the pulse on time results in wire breakage. It is evident from the graph that no wire

Table 7. Standard deviation, criterion value and weighted value

Criteria	Standard deviation, σ	Quantity of information, d_q	Weight value, W_q
MR	0.2779	0.3200	0.4549
Surface roughness, R_a	0.3329	0.3833	0.5450

MR, machining rate

Table 8. Normalised decision matrix for the CRITIC and SAW methods

Normalised values by the CRITIC method		Normalised values by the SAW method		B_p	Ranking
0.3421	0.3379	0.2230	0.2385	0.7925	10
0.3421	0	0.2230	0.2514	0.7675	14
1	0.0814	0.3323	0.2483	0.9229	1
0.1842	1	0.1967	0.2131	0.8144	9
0.6447	0.0104	0.2733	0.2510	0.8370	6
0.6315	0.026	0.2711	0.2504	0.8351	7
0.3684	0.6984	0.2273	0.2247	0.8284	8
0.1184	0.6984	0.1858	0.2247	0.7715	13
0.3947	0.1265	0.2317	0.2465	0.7885	11
0.1184	0.3899	0.1858	0.2365	0.7457	15
0.6842	0.3812	0.2798	0.2368	0.8737	4
0.7763	0.6759	0.2951	0.2255	0.9192	2
0.0789	0.4558	0.1792	0.234	0.7420	16
0.2105	0.6499	0.2011	0.2265	0.7882	12
0.6184	0.9826	0.2689	0.2138	0.9115	3
0	0.1143	0.1661	0.2470	0.6978	18
0.1578	0.1889	0.1924	0.2442	0.7392	17
0.3947	0.7365	0.2317	0.2232	0.8377	5

CRITIC, CRiteria Importance Through Intercriteria Correlation; SAW, simple additive weighting

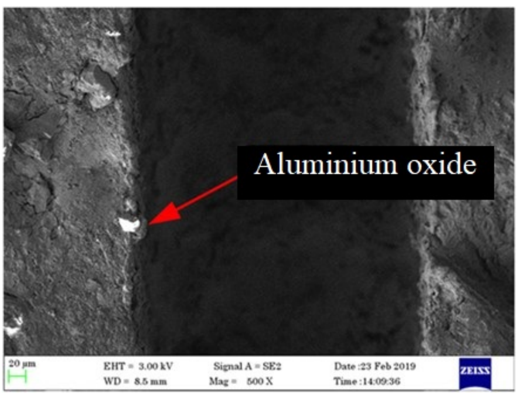

Fig. 12. SEM graph of the machined slot at an experimental condition of 70 V, 7 mm/min, 310 A, 120 µs (ON_T) and 50 µs. SEM, scanning electron microscopy

breakage has occurred at lower pulse on time; and with increase in the pulse on time, the frequency of breakage increases. It is due to the fact that increase in pulse on time increases the discharge rate. The high frequency discharge increases the erosion and breaking of the wire. Another important factor for the cause of wire breakage is short circuit. Short circuits take place due to longer pulse on time, and the material removed from the workpiece creates the conductive bridge, resulting in unwanted sparking. Hence, an increased frequency of sparking contributes towards frequent breaking of wires.

On comparing the other parameter, the pulse off time (OFF_T) has not attained complete machining, as shown in Figure 11. In AMMCs workpiece, reinforcements are used to increase the strength of the material, and this amalgamation of particles causes clustering of particles and weak matrix-reinforcement bonding. Therefore, when a proper gap is not maintained during wire travel, this results in frequent wire breakages owing to the pro-

Table 9. ANOVA results for MR and R_a

Source of variation	Degree of freedom	Sum of squares	Mean sum of squares	*F* value	*p* value	% of Contribution
Surface roughness						
Voltage (V)	2	0.04409	0.022046	0.43	0.669	7.03
Wire feed rate	2	0.03265	0.016323	0.32	0.739	5.21
Current	2	0.03130	0.015649	0.30	0.748	4.99
Pulse on time	**2**	0.14463	0.072317	1.40	0.308	23.06
Pulse off time	**2**	0.01268	0.006342	0.12	0.886	2.02
Error	7	0.36188	0.051698			57.69
Total	17	0.62724				100
MR						
Voltage (V)	2	0.16103	0.080517	9.28	0.011	21.23
Wire feed rate	2	0.36270	0.181350	20.90	0.001	47.82
Current	2	0.01343	0.006717	0.77	0.497	1.77
Pulse on time	**2**	0.01710	0.008550	0.99	0.420	2.25
Pulse off time	**2**	0.14343	0.071717	8.26	0.014	18.91
Error	10	0.06075	0.008679			8.01
Total	17	0.75845				100.00

ANOVA, analysis of variance; MR, machining rate

trusion of reinforcement particles and the resultant sharp corners. SEM image of the incomplete slot machined at the parameter combination of 70 V, 7 mm/min, 310 A, 120 μs (ON_T) and 50 μs is shown in Figure 12, and the time for the first wire breakage is found to be 120 μs (ON_T). The presence of protruded Al_2O_3 is noticed on the wire travel zone.

As per Eqs (1)–(8), the weights for the criteria (MR and R_a) were calculated as 0.4549 and 0.5450, respectively, and are presented in Table 7. Table 8 shows the normalised values of MR and R_a determined based on Eqs (1)–(8). Based on the CRITIC and SAW methods, the parameter combination of 30 V, 7 mm/min, 30 A, 120 μs (ON_T) and 70 μs (OFF_T) is the first ranked for higher MR and lower R_a. Additionally, 30 V, 7 mm/min, 20 A, 110 μs (ON_T) and 50 μs (OFF_T) is the second ranked combination. The results of the ANOVA are represented in Table 9. The ANOVA for MR and R_a shows that wire feed rate and voltage contribute 47.82% and 21.23%, respectively, for MR; and pulse on time shows 23.06% for surface roughness.

4. Conclusions

For the first time, the WEDM of a new kind of AMMC produced using scrap aluminium alloy wheels reinforced with 5% alumina in a stir-squeeze casting setup is investigated. The experimental study was performed by varying one parameter at a time and five control parameters were used, namely voltage (V), wire feed (F_w), current (I_p), pulse on time (ON_T) and pulse off time (OFF_T). For the parameter combination of 30 V, 7 mm/min, 30 A, 120 μs (ON_T) and 70 μs, the time taken to machine the slot is found to be 304 s; moreover, no breakage of wire is observed from employing this parametric combination.

However, with increase in the voltage, wire breakage occurs, the earliest being 22 s at 70 V. The completion of slot machining without breakage of wire is made possible using the parameter combination of 70 V, 3 mm/min, 30 A, 120 μs (ON_T) and 70 μs in 435 s. The wire breakage is observed at the earliest time of 15 s at the highest feed rate of 7 m/min. The lowest value of peak current at which a wire breakage is observed is noted at 30 A, and 727 s is the time taken to machine the slot up to a depth of 9.8 mm. The two slots were successfully completed at pulse on time of 100 μs and

105 μs without wire breakage, and the time taken for the completion of the slots was, respectively, 1,115 s and 847 s. The best parameter combination for higher MR and lower R_a is 30 V, 7 mm/min, 30 A, 120 μs (ON_T) and 70 μs (OFF_T). ANOVA results predict that wire feed rate and voltage contribute 47.82% and 21.23%, respectively, for MR; and pulse on time shows a 23.06% influence on surface roughness. The experimental investigations conducted in the present study indicate that, to avoid the wire breakage phenomenon and ensure a stable machining, the optimum WEDM parameters can be obtained at the lowest values for all concerned parameters: voltage, wire feed rate and pulse on time. In further research, it is planned to conduct the experiments based on hard-to-cut materials and to try various optimisation techniques to improve the machining performance of WEDM.

Abbreviations

AMMC, aluminium metal matrix composite; ANOVA, analysis of variance; B_p, highest ranking for the MR and surface roughness; EDS, energy-dispersive X-ray spectrometry; F_w, wire feed rate; I_p, current; KW, kerf width; MMC, metal matrix composite; MR, machining rate; MRR, material removal rate; OFF_T, pulse off time; ON_T, pulse on time; R_a, surface roughness; SAAWs, scrap aluminium alloy wheels; SEM, scanning electron microscopy; V_s, servo voltage; WEDM, wirecut electrical discharge machining.

References

[1] Phate MR, Toney SB. Modeling and prediction of WEDM performance parameters for Al/SiCp MMC using dimensional analysis and artificial neural network. Eng Sci Technol Int J. 2019;22(2):468–76. https://doi.org/10.1016/j.jestch.2018.12.002

[2] Karthik S, Prakash KS, Gopal PM, Jothi S. Influence of materials and machining parameters on WEDM of Al/AlCoCrFeNiMo0. 5 MMC. Mater Manuf Process. 2019;34(7):759–68. https://doi.org/10.1080/10426914.2019.1594250

[3] Ramraji K, Rajkumar K, Selvakumar G. Investigations on the influence of particle reinforcement and wire materials on the surface quality and machining characteristics of AA6061-TiB_2 alloy in WEDM. Surf Topogr Metrol Prop. 2021;9(3):035029.

[4] Chen Z, Zhou H, Wu C, Zhang G, Yan H. A new wire electrode for improving the machining characteristics of high-volume fraction SiCp/Al composite in WEDM. Materials. 2022;15(12):4098.

[5] Garg SK, Manna A, Jain A. Investigation and analysis of surface veracity and parametric aspects during wireEDM of Al/ZrO_2 (p)-metal matrix composite. Arab J Sci Eng. 2022; 47:8417–38. https://doi.org/10.1007/s13369-021-05531-9

[6] Prakash JU, Sivaprakasam P, Garip I, Juliyana SJ, Elias G, Kalusuraman G, et al. Wire electrical discharge machining (WEDM) of hybrid composites (Al-Si12/B_4C/fly Ash). J Nanomater. 2021; 2021:1–10. https://doi.org/10.1155/2021/2503673

[7] Mythili T, Thanigaivelan R. Optimization of wire EDM process parameters on Al6061/Al_2O_3 composite and its surface integrity studies. Bull Pol Acad Sci Tech Sci. 2020; 68:1403–12.

[8] Vijay Praveen D, Ranga Raju D, Raju J. Assessment of optimal parameters of wire EDM on Ni-coated Al_2O_3p/AA7075 MMCs using PCA coupled GRA. Arab J Sci Eng. 2021;46(8):7953–66.

[9] Juliyana SJ, Prakash JU. Optimization of machining parameters for wire EDM of AMCs (LM5/ZrO_2) using Taguchi technique. INCAS Bull. 2022;14(1):57–68.

[10] Lenin N, Sivakumar M, Selvakumar G, Rajamani D, Sivalingam V, Gupta MK, et al. Optimization of process control parameters for WEDM of Al-LM25/Fly Ash/B4C hybrid composites using evolutionary algorithms: a comparative study. Metals. 2021;11(7):1105.

[11] Kavimani V, Prakash KS, Thankachan T. Multi-objective optimization in WEDM process of graphene–SiC-magnesium composite through hybrid techniques. Measurement. 2019; 145:335–49.

[12] Lajis MA, Ahmad A, Yusuf NK, Azami AH, Wagiman A. Mechanical properties of recycled aluminium chip reinforced with alumina (Al_2O_3) particle. Mater Sci Eng Technol; 2^{nd} International Conference on Mechanical, Manufacturing and Process Plant Engineering (ICMMPE-2016). 2017; 48:306–10. https://doi.org/10.1002/mawe.201600778

[13] Doreswamy D, Bongale AM, Piekarski M, Bongale A, Kumar S, Pimenov DY, et al. Optimization and modeling of material removal rate in wire-EDM of silicon particle reinforced Al6061 composite. Materials. 2021;14(21):6420.

[14] Krishnan PK, Christy JV, Arunachalam R, Mourad AHI, Muraliraja R, Al-Maharbi M, et al. Production of aluminum alloy-based metal matrix composites using scrap aluminum alloy and waste materials: influence on microstructure and mechanical properties. J Alloys Compd. 2019; 784:1047–61.

[15] Sathish T, Mohanavel V, Ansari K, Saravanan R, Karthick A, Afzal A, et al. Synthesis and characterization of mechanical properties and wire cut EDM process parameters analysis in AZ61 magnesium alloy + B_4C + SiC. Materials. 2021;14(13):3689. https://doi.org/10.3390/ma14133689

[16] Thiraviam R, Ravisankar V, Kumar P, Thanigaivelan R, Arunachalam R. A novel approach for the production and characterisation of aluminium–alumina hybrid metal matrix composites. Mater Res Express. 2020;7(4):046512.

[17] Sharma P, Chakradhar D, Narendranath S. Effect of wire material on productivity and surface integrity of WEDM-processed Inconel 706 for aircraft application. J Mater Eng Perform. 2016;25(9):3672–81. https://doi.org/10.1007/s11665-016-2216-z

[18] Kumar N, Kumari S, Abhishek K, Nandi G, Ghosh N. Study on various parameters of WEDM using different optimization techniques: a review. Mater Today Proc. 2022; 62:4018–24.

[19] Saha S, Maity SR, Dey S. Particle swarm optimization-based search for optimal operating condition in WEDM operation of A286 superalloy. In: Recent advancements in mechanical engineering. Singapore: Springer; 2023. pp. 577–85.

[20] Kalita K, Ghadai RK, Chakraborty SA. comparative study on multi-objective Pareto optimization of WEDM process using nature-inspired metaheuristic algorithms. Int J Interact Des Manuf. 2022; 11:1–8.

Received 2022-09-27
Accepted 2022-11-21